

# All Fermion Masses and Mixings in an Intersecting D-brane World

VAN E. MAYES

*Department of Physical and Applied Sciences,  
University of Houston-Clear Lake  
Houston, TX 77058, USA*

## Abstract

It is shown that neutrino mixing angles which are consistent with current experimental observations may be naturally obtained in a Pati-Salam model constructed from intersecting D6 branes on a  $T^6/(\mathbb{Z}_2 \times \mathbb{Z}_2)$  orientifold. The Dirac mass matrices in the model are naturally the same as those which are obtained by imposing a  $\Delta(27)$  flavor symmetry, which allows for near-tribimaximal mixing in the neutrino sector. In addition, it is possible to obtain the correct mass matrices for quarks and charged leptons, as well as nearly the correct CKM matrix. An RGE analysis of the neutrino mass parameters, including the seesaw mechanism assuming a specific form for the right-handed neutrino mass matrix is performed, and it is found that the neutrino mixing angles at the electroweak scale are  $\theta_{12} = 35.0^\circ$ ,  $\theta_{23} = 47.1^\circ$ , and  $\theta_{13} = 8.27^\circ$ . In addition, the neutrino mass-squared differences are found to be  $\Delta m_{32}^2 = 0.00252 \text{ eV}^2$  and  $\Delta m_{21}^2 = 0.0000739 \text{ eV}^2$  with  $m_1 = 0.0146 \text{ eV}$ ,  $m_2 = 0.0170 \text{ eV}$ , and  $m_3 = 0.0530 \text{ eV}$ . These results depend slightly upon the scale at which the RGE running goes from being that of the MSSM to that of the SM, which we interpret to be the lightest stop mass. The best agreement with experimental data is for  $\tilde{m}_{t_1} \approx 4.28 \text{ TeV}$ . This suggests that the superpartners which produce the strongest signal in a hadron collider are just out of reach at the LHC.

# 1 Introduction

The SM exhibits an intricate pattern of mass hierarchies and mixings between the different generations of fermions. The pattern of neutrino mixings is one of the most interesting aspects of neutrino physics today. In contrast to the small quark mixing angles, the mixing angles between neutrinos appear to be quite large. The observation of neutrino oscillations suggests that there are small mass differences between the different neutrino mass states. At present, the masses and mixing angles for both quarks and leptons remains completely unexplained, as well as the question of why they are so different from one another.

In recent years, precision measurements of the neutrino mixing angles as well as the squares of the mass differences between neutrinos have been made by several experiments. The best estimate of the difference in the squares of the masses of mass eigenstates 1 and 2 was published by KamLAND in 2005:  $\Delta m_{21}^2 = 0.0000739_{-0.20}^{+0.21} \text{ eV}^2$  [1, 2, 3, 4]. In addition, the MINOS experiment measured oscillations from an intense muon neutrino beam, determining the difference in the squares of the masses between neutrino mass eigenstates 2 and 3. Current measurements indicate  $\Delta m_{32}^2 = 0.0027 \text{ eV}^2$  [2, 3, 4], consistent with previous results from Super-Kamiokande [5]. In addition, recent analysis of cosmological results constrains the sum of the three neutrino masses to be  $\lesssim 0.12 \text{ eV}$  [6], while additional analysis of combined data sets results in  $0.15 \text{ eV}$  [7] and  $0.19 \text{ eV}$  [8] for the upper limit. Older analyses set the upper limit slightly higher at  $0.3 \text{ eV}$  [9, 10, 11].

The lepton mixing matrix or PMNS matrix may be parameterized as

$$U_{PMNS} = \begin{pmatrix} c_{12}c_{13} & s_{12}c_{13} & s_{13}e^{-i\delta_{CP}} \\ -s_{12}c_{23} - c_{12}s_{23}s_{13}e^{i\delta_{CP}} & c_{12}c_{23} - s_{12}s_{23}s_{13}e^{i\delta_{CP}} & s_{23}c_{13} \\ s_{12}s_{23} - c_{12}c_{23}s_{13}e^{i\delta_{CP}} & -c_{12}s_{23} - s_{12}c_{23}s_{13}e^{i\delta_{CP}} & c_{23}c_{13} \end{pmatrix}, \quad (1)$$

where  $s_{ij}$  and  $c_{ij}$  denote  $\sin \theta_{ij}$  and  $\cos \theta_{ij}$  respectively, while  $\delta_{CP}$  is a  $CP$ -violating phase.

The current best-fit values for the mixing angles from direct and indirect experiments are, using normal ordering [2, 3, 4],

$$\begin{aligned} \theta_{12} &= 33.82_{-0.76}^{+0.78} \text{ }^\circ, \\ \theta_{23} &= 49.6_{-1.2}^{+1.0} \text{ }^\circ \\ \theta_{13} &= 8.61_{-0.13}^{+0.13} \text{ }^\circ \\ \delta_{CP} &= 215_{-29}^{+40} \text{ }^\circ \end{aligned} \quad (2)$$

One of the most studied patterns of neutrino mixing angles is the so-called tribimaximal mixing of the form

$$U_{TB} \sim \begin{pmatrix} \sqrt{\frac{2}{3}} & \sqrt{\frac{1}{3}} & 0 \\ -\sqrt{\frac{1}{6}} & \sqrt{\frac{1}{3}} & -\sqrt{\frac{1}{2}} \\ -\sqrt{\frac{1}{6}} & \sqrt{\frac{1}{3}} & \sqrt{\frac{1}{2}} \end{pmatrix}, \quad (3)$$

which were consistent with early data. However, the measurement of a nonzero  $\theta_{13}$  by Data Bay [12] and Double Chooz [13], and confirmed by RENO [14] has now ruled out these mixing patterns. Although tribimaximal mixing is currently ruled out by experimental data, it still may

be viewed as a zeroth-order approximation to more general forms of the PMNS matrix which are also consistent with the data. Thus, it is still of great importance to understand the origin of tribimaximal mixing.

In particular, it was shown also by Ma that mass matrices leading to tribimaximal and near-tribimaximal mixing may be generated by imposing a flavour symmetry such as **A4** [15] or  $\Delta(27)$  [16]. Specifically, a mass matrix of the form

$$\mathcal{M}_\nu \sim \begin{pmatrix} Y & X & X \\ X & y & x \\ X & x & y \end{pmatrix}, \quad (4)$$

obtained by imposing an **A4** flavour symmetry leads to tribimaximal mixing, while mass matrices of the form

$$\mathcal{M}_\nu \sim \begin{pmatrix} f_1 v_1 & f_2 v_3 & f_2 v_2 \\ f_2 v_3 & f_1 v_2 & f_2 v_1 \\ f_2 v_2 & f_2 v_1 & f_1 v_3 \end{pmatrix}, \quad (5)$$

obtained by imposing an  $\Delta(27)$  flavour symmetry may lead to near-tribimaximal mixing as  $\Delta(27)$  contains **A4** as a subgroup. Although generating mass matrices of this form through a flavour symmetry is very elegant and does provide some insight into the origin of the neutrino mixing angles, the origin of the flavour symmetries required for this in a fundamental theory has yet to be explained.

String theory is a leading candidate for such a theory. The main challenge of string phenomenology is to exhibit at least one string vacuum that describes the physics of our universe in detail. Despite progress in this direction, this has not yet been completely achieved. In the past two decades, a promising approach to model building has emerged involving compactifications with D branes on orientifolds (for reviews, see [17, 18, 19, 20]). In such models chiral fermions—an intrinsic feature of the Standard Model (SM)—arise from configurations with D branes located at transversal orbifold/conifold singularities [21] and strings stretching between D branes intersecting at angles [22, 23] (or, in its T-dual picture, with magnetized D branes [24, 25, 26]). A number of non-supersymmetric intersecting D-brane models have been constructed that strongly resemble the SM.

However, non-supersymmetric low-energy limits of string theory suffer from internal inconsistencies of noncanceled NS-NS tadpoles, yielding models that destabilize the hierarchy of scales [27]. A resolution of these issues necessarily requires  $\mathcal{N} = 1$  supersymmetry. The first semirealistic models that preserve the latter were built in Type IIA theory on a  $T^6/(\mathbb{Z}_2 \times \mathbb{Z}_2)$  orientifold [28, 29]. Subsequently, intersecting D-brane models based on SM-like, Pati-Salam [30], and SU(5) [31] gauge groups were constructed within the same framework and systematically studied in Refs. [32, 33, 34, 35, 36, 37]<sup>1</sup>. The statistics of 3- and 4-generation models was studied in [40, 41]. Phenomenologically interesting models have also been constructed on a  $T^6/(\mathbb{Z}_6)$  orientifold [42]. In addition, several different models with flipped SU(5) [43] have been suggested within intersecting D-brane scenarios [44, 45], as well as models with interesting discrete-group flavor structures [46].

Within the framework of D-brane modeling it was demonstrated that the Yukawa matrices  $Y_{abc} \sim \exp(-A_{abc})$  arise from worldsheet areas  $A_{abc}$  spanning D branes (labeled by  $a, b, c$ ) supporting fermions and Higgses at their intersections [23, 47]. This pattern naturally encodes

---

<sup>1</sup>see [38] and [39] for heterotic constructions of Pati-Salam models.

the hierarchy of Yukawa couplings. However, for most string constructions, Yukawa matrices are of rank one. In the case of D-brane models built on toroidal orientifolds, this result can be traced to the fact that not all of the intersections at which the SM fermions are localized occur on the same torus. To date only one three-generation model is known in which this problem has been overcome [48], and for which one can obtain mass matrices for quarks and leptons that nearly reproduce experimental values. Additionally, this model exhibits automatic gauge coupling unification at the string scale, and all extra matter can be decoupled. It should be commented that the rank-1 problem for toroidal models can also potentially be solved by D-brane instantons [49, 50, 51]. However, the conditions for including these nonperturbative effects are very constraining, and at present there are no concrete realizations in the literature in which all constraints may be satisfied.

In the following, shown that neutrino mixing angles which are consistent with current experimental observations may be naturally obtained in a Pati-Salam model constructed from intersecting D6 branes on a  $T^6/(\mathbb{Z}_2 \times \mathbb{Z}_2)$  orientifold. The Dirac mass matrices in the model are naturally the same as those which are obtained by imposing a  $\Delta(\mathbf{27})$  flavor symmetry, which allows for near-tribimaximal mixing in the neutrino sector. In addition, it is possible to obtain the correct mass matrices for quarks and charged leptons, as well as nearly the correct CKM matrix. An RGE analysis of the neutrino mass parameters, including the seesaw mechanism assuming a specific form for the right-handed neutrino mass matrix is performed, and it is found that the neutrino mixing angles at the electroweak scale are  $\theta_{12} = 35.0^\circ$ ,  $\theta_{23} = 47.1^\circ$ , and  $\theta_{13} = 8.27^\circ$ . In addition, the neutrino mass-squared differences are found to be  $\Delta m_{32}^2 = 0.00252 \text{ eV}^2$  and  $\Delta m_{21}^2 = 0.0000739 \text{ eV}^2$  with  $m_1 = 0.0146 \text{ eV}$ ,  $m_2 = 0.0170 \text{ eV}$ , and  $m_3 = 0.0530 \text{ eV}$ . These results depend slightly upon the scale at which the RGE running goes from being that of the MSSM to that of the SM, which we interpret to be the lightest stop mass. The best agreement with experimental data is for  $\tilde{m}_{t_1} \approx 4.28 \text{ TeV}$ . This suggests that the superpartners which produce the strongest signal in a hadron collider are just out of reach at the LHC.

## 2 A Realistic MSSM

The configuration of D branes must obey a number of conditions in order to be a consistent model of particle physics. First, the RR tadpoles vanish via the Gauss' law cancellation condition for the sum of D-brane and cross-cap RR-charges [19, 52]:

$$\sum_{\alpha \in \text{stacks}} N_\alpha (\pi_\alpha + \pi_{\alpha^*}) - 4\pi_{O6} = 0, \quad (6)$$

written in terms of the three-cycles  $\pi_\alpha = (n_1^\alpha, l_1^\alpha) \times (n_2^\alpha, l_2^\alpha) \times (n_3^\alpha, 2^{-\beta} l_3^\alpha)$  that wrap  $(n_j^\alpha, m_j^\alpha)$  times the fundamental cycles  $([a_j], [b_j])$  of the factorizable six-torus  $T^6 = \prod_{j=1}^3 T_{(j)}^2$ . Here, the first two two-tori are rectangular:  $l_j^\alpha = m_j^\alpha$  ( $j = 1, 2$ ), while the third two-torus can be rectangular ( $\beta=0$ ), or tilted such that  $l_3^\alpha = 2m_j^\alpha + n_j^\alpha$  and  $\beta = 1$ . In the T-dual picture the tilt of the third cycle  $[a'_3] = [a_3] + \frac{1}{2}[b_3]$  corresponds to turning on a non-zero NS-NS two-form  $B$  field. However, it becomes nondynamical under the requirement of its invariance under the orientifold projection  $\Omega\mathcal{R}$  [53]. As a consequence, its flux can admit only two discrete values, resulting in two discrete values for  $\beta$ . Each two-torus possesses the complex structure modulus  $\chi_j = R_2^{(j)}/R_1^{(j)}$  built from its radii  $R_1^{(j)}$  and  $R_2^{(j)}$ .  $\mathcal{N} = 1$  supersymmetry, which is favored for reasons of underlying

Table 1: General spectrum for intersecting D6 branes at generic angles, where  $I_{aa'} = -2^{3-\beta} \prod_{i=1}^3 (n_a^i l_a^i)$ , and  $I_{aO6} = 2^{3-\beta} (-l_a^1 l_a^2 l_a^3 + l_a^1 n_a^2 n_a^3 + n_a^1 l_a^2 n_a^3 + n_a^1 n_a^2 l_a^3)$ .  $\mathcal{M}$  is the multiplicity, and  $a_S$  and  $a_A$  denote the symmetric and antisymmetric representations of  $U(N_a/2)$ , respectively.

Sector	Representation
$aa$	$U(N_a/2)$ vector multiplet and 3 adjoint chiral multiplets
$ab + ba$	$\mathcal{M}(\frac{N_a}{2}, \frac{\bar{N}_b}{2}) = I_{ab} = 2^{-\beta} \prod_{i=1}^3 (n_a^i l_b^i - n_b^i l_a^i)$
$ab' + b'a$	$\mathcal{M}(\frac{N_a}{2}, \frac{N_b}{2}) = I_{ab'} = -2^{-\beta} \prod_{i=1}^3 (n_a^i l_b^i + n_b^i l_a^i)$
$aa' + a'a$	$\mathcal{M}(a_S) = \frac{1}{2}(I_{aa'} - \frac{1}{2}I_{aO6})$ ; $\mathcal{M}(a_A) = \frac{1}{2}(I_{aa'} + \frac{1}{2}I_{aO6})$

consistent low-energy theories of particle physics as well as for stability of D-brane configurations, is preserved by choosing the angles between the D-brane stacks and orientifold planes to obey the condition [28, 29]

$$\theta_1^\alpha + \theta_2^\alpha + \theta_3^\alpha = 0 \pmod{2\pi}, \quad (7)$$

with  $\theta_j^\alpha = \arctan(2^{-\beta_j} \chi_j l_j^\alpha / n_j^\alpha)$  and  $\beta_{1,2} = 0$  and  $\beta_3 = \beta$ . This condition can be written in terms of wrapping numbers satisfying the two equations

$$\begin{aligned} x_A \tilde{A}_a + x_B \tilde{B}_a + x_C \tilde{C}_a + x_D \tilde{D}_a &= 0, \\ A_a/x_A + B_a/x_B + C_a/x_C + D_a/x_D &< 0, \end{aligned} \quad (8)$$

where

$$\begin{aligned} \tilde{A}_a &= -l_a^1 l_a^2 l_a^3, & \tilde{B}_a &= l_a^1 n_a^2 n_a^3, & \tilde{C}_a &= n_a^1 l_a^2 n_a^3, & \tilde{D}_a &= n_a^1 n_a^2 l_a^3, \\ A_a &= -n_a^1 n_a^2 n_a^3, & B_a &= n_a^1 l_a^2 l_a^3, & C_a &= l_a^1 n_a^2 l_a^3, & D_a &= l_a^1 l_a^2 n_a^3, \end{aligned} \quad (9)$$

and  $x_A, x_B, x_C$ , and  $x_D$  are the complex structure parameters [35], where  $x_A = \lambda$ ,  $x_B = \lambda \cdot 2^{\beta_2+\beta_3} / \chi_2 \chi_3$ ,  $x_C = \lambda \cdot 2^{\beta_1+\beta_3} / \chi_1 \chi_3$ ,  $x_D = \lambda \cdot 2^{\beta+\beta_2} / \chi_1 \chi_2$ , and  $\lambda$  is a positive parameter that puts the parameters  $A, B, C$ , and  $D$  on equal footing. Furthermore, the consistency of the model is further ensured by the K-theory conditions [54, 55], which imply the cancellation of the  $Z_2$  charges carried by D branes in orientifold compactifications in addition to the vanishing of the total homological charge exhibited by Eq. (6). In the present case, nonvanishing torsion charges are avoided by considering stacks with an even number of D branes, *i.e.*,  $N_\alpha \in 2\mathbb{Z}$ .

Imposing these constraints, we present the D6-brane configurations, intersection numbers, and complex structure parameters of the model in Table 2, and the resulting spectrum in Table 3, with formulas for calculating the multiplicity of states in bifundamental, symmetric, and antisymmetric states shown in Table 1. Models with different numbers of generations may be obtained for different values of the wrapping number  $n_g$  as well as the third-torus tilt parameter  $\beta$ . The observable sector of the models then has the gauge symmetry and matter content of an  $(N_g = 2^{1-\beta} n_g)$ -generation SM with an extended Higgs sector. The extra matter in the models consists of matter charged under the hidden-sector gauge groups, and vectorlike matter between pairs of branes that do not intersect, as well as the chiral adjoints associated with each stack of branes. In addition, one has matter in the symmetric triplet representation of  $SU(2)_L$  as well as

additional singlets. In order to have just the MSSM at low energies, the gauge couplings must unify at some energy scale, and all extra matter besides the MSSM states must become massive at high-energy scales. Furthermore, one requires just one pair of Higgs doublets.

The resulting models have gauge symmetry  $[U(4)_C \times U(2)_L \times U(2)_R]_{\text{observable}} \times [\text{USp}(2^{2-\beta}(4 - n_g))^2 \times \text{USp}(2^{2-\beta})^2]_{\text{hidden}}$ . The hidden sector, as well as the set of complex structure parameters required to preserve  $\mathcal{N} = 1$  supersymmetry, is different in each of the models with different numbers of generations. In particular, in the tilted case two of the hidden-sector gauge groups fall out in going from three-generation to four-generation models. The non-Abelian chiral anomalies vanish as a consequence of the RR tadpole condition (6). The chiral anomalies from the three global U(1)s of  $U(4)_C$ ,  $U(2)_L$ , and  $U(2)_R$  inducing couplings of the form  $A_\alpha \wedge F_\beta^2$ , with  $A$  and  $F$  referring to Abelian and non-Abelian gauge fields, respectively, read [56]

$$\mathcal{A}^{\text{chiral}} = \frac{1}{2} \sum_{\alpha, \beta} N_\alpha (I_{\alpha\beta} - I_{\alpha^*\beta}) A_\alpha \wedge F_\beta^2, \quad (10)$$

However, these anomalies cancel against the couplings induced by RR fields via the Green-Schwarz mechanism [56]:

$$\mathcal{A}^{\text{RR}} = 8n_g A_a \wedge (F_c^2 - F_b^2) + 4n_g A_b \wedge F_a^2 - 4n_g A_c \wedge F_a^2, \quad (11)$$

such that  $\mathcal{A}^{\text{chiral}} + \mathcal{A}^{\text{RR}} = 0$ . The gauge fields  $A_\alpha$  of these U(1)s receive masses via linear  $\sum_\ell c_\ell^\alpha B_2^\ell \wedge A_\alpha$  couplings in the ten-dimensional action, with the massless modes given by  $\ker(c_\ell^\alpha)$ . The latter is trivial in the present model, which means that the effective gauge symmetry of the observable sector is  $SU(4)_C \times SU(2)_L \times SU(2)_R$ .

In order to break the gauge symmetry of the observable sector down to the SM, we split the  $a$  stack of D6 branes on the first two-torus into stacks  $a_1$  and  $a_2$  with  $N_{a_1} = 6$  and  $N_{a_2} = 2$  D6 branes, and similarly split the  $c$  stack of D6 branes into stacks  $c_1$  and  $c_2$  such that  $N_{c_1} = 2$  and  $N_{c_2} = 2$  as shown in Fig. 1. The process of brane-splitting corresponds to giving a vacuum expectation value (VEV) to the chiral adjoint fields associated with each stack, which are open-string moduli. The gauge symmetry subsequently breaks down to  $SU(3)_C \times SU(2)_L \times U(1)_{I_{3R}} \times U(1)_{B-L}$ , where the  $U(1)_{I_{3R}}$  and  $U(1)_{B-L}$  gauge bosons remain massless. The  $U(1)_{I_{3R}} \times U(1)_{B-L}$  gauge symmetry may then be broken to  $U(1)_Y = \frac{1}{2}U(1)_{B-L} + U(1)_{I_{3R}}$  by giving VEVs to the vectorlike particles with the quantum numbers  $(\mathbf{1}, \mathbf{1}, 1/2, -1)$  and  $(\mathbf{1}, \mathbf{1}, -1/2, 1)$  under the  $SU(3)_C \times SU(2)_L \times U(1)_{I_{3R}} \times U(1)_{B-L}$  gauge symmetry arising from  $a_2 c_1'$  intersections. The full gauge symmetry of the models is then  $SU(3)_C \times SU(2)_L \times U(1)_Y \times [\text{USp}[2^{2-\beta}(4 - n_g)]^2 \times \text{USp}(2^{2-\beta})^2]$ , with the hypercharge given by

$$Q_Y = \frac{1}{6} (Q_{a_1} - 3Q_{a_2} - 3Q_{c_1} + 3Q_{c_2}), \quad (12)$$

where the  $a$ -stack charges provide  $Q_{B-L}$  and the  $c$ -stack charges provide  $Q_{3R}$ .

The gauge coupling constant associated with a stack  $\alpha$  is given by

$$g_{\text{D6}\alpha}^{-2} = |\Re(f_\alpha)|, \quad (13)$$

where  $f_\alpha$  is the holomorphic gauge kinetic function associated with stack  $\alpha$ , given [19, 27] in terms of NS-NS fields by:

$$f_\alpha = \frac{1}{4\kappa_\alpha} [n_1^\alpha n_2^\alpha n_3^\alpha s - 2^{-\beta} n_1^\alpha l_2^\alpha l_3^\alpha u^1 - 2^{-\beta} n_2^\alpha l_1^\alpha l_3^\alpha u^2 - n_3^\alpha l_1^\alpha l_2^\alpha u^3], \quad (14)$$

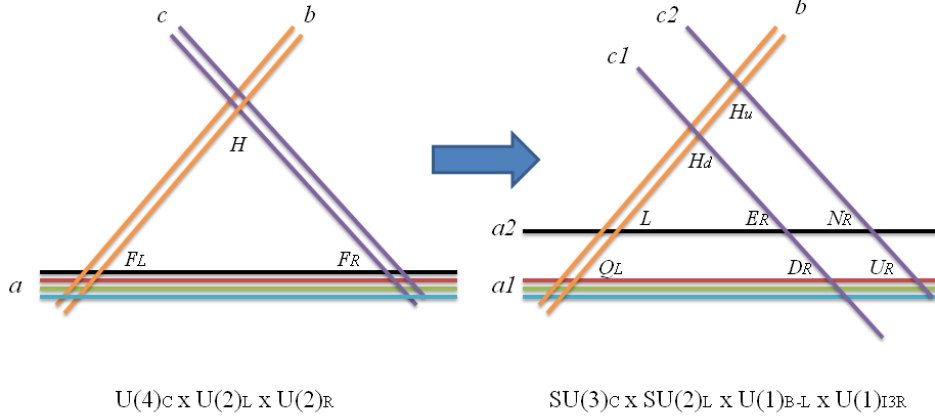


Figure 1: Breaking of the effective gauge symmetry via D-brane splitting. This process corresponds to assigning VEVs to adjoint scalars, which arise as open-string moduli associated with the positions of stacks  $a$  and  $c$  in the internal space.

where  $\kappa_\alpha = 1$  for  $SU(N_\alpha)$  and  $\kappa_\alpha = 2$  for  $USp(2N_\alpha)$  or  $SO(2N_\alpha)$  gauge groups. The holomorphic gauge kinetic function associated with SM hypercharge  $U(1)_Y$  is then given by taking a linear combination of the holomorphic kinetic gauge functions from all of the stacks [57]:

$$f_Y = \frac{1}{6}f_{a_1} + \frac{1}{2}(f_{a_2} + f_{c_1} + f_{c_2}). \quad (15)$$

Note that in Eq. (14), the four-dimensional dilaton  $s$  and complex structure moduli  $u^i$  refer to the supergravity basis. These moduli must be stabilized, and gaugino condensation of the effective Veneziano-Yankielowicz Lagrangian [58] provides an example of such a mechanism [59]. Gaugino condensation in the hidden sectors can play an important role in moduli stabilization, and it might provide a top-down reason why three generations is preferred over four.

From the complex structure parameters, the complex structures  $U^i$  are determined to be

$$U^1 = n_g \cdot i, \quad U^2 = i, \quad U^3 = -\beta + i. \quad (16)$$

The dilaton and complex structure moduli are then given in the supergravity basis by<sup>2</sup>

$$\begin{aligned} \text{Re}(s) &= \frac{1}{(2^\beta n_g)^{1/2}} \frac{e^{-\phi_4}}{2\pi}, & \text{Re}(u^1) &= \left(\frac{2^\beta}{n_g}\right)^{1/2} \frac{e^{-\phi_4}}{2\pi}, \\ \text{Re}(u^2) &= (2^\beta n_g)^{1/2} \frac{e^{-\phi_4}}{2\pi}, & \text{Re}(u^3) &= \frac{1}{(2^\beta n_g)^{1/2}} \frac{e^{-\phi_4}}{2\pi}, \end{aligned} \quad (17)$$

<sup>2</sup>See, e.g., footnote 5 of Ref. [57] for the relation between these and complex structures  $U^i$ .

Table 2: D6-brane configurations and intersection numbers for a series of Pati-Salam models with  $2^{1-\beta}n_g$  generations on a Type IIA  $T^6/(\mathbb{Z}_2 \times \mathbb{Z}_2)$  orientifold, where the tadpole conditions are satisfied without introducing fluxes. The parameter  $\beta$  can be zero or one if the third torus is untilted or tilted respectively, while the wrapping number  $n_g$  may take the values 1, 2, 3, or 4. The complete gauge symmetry is  $[U(4)_C \times U(2)_L \times U(2)_R]_{\text{observable}} \times \{\text{USp}[2^{2-\beta}(4-n_g)]^2 \times \text{USp}(2^{2-\beta})^2\}_{\text{hidden}}$ , and the complex structure parameters that preserve  $\mathcal{N} = 1$  supersymmetry are  $x_A = x_B = n_g \cdot x_C = n_g \cdot x_D$ . The parameters  $\beta_i^g$  give the  $\beta$ -functions for the hidden-sector gauge groups.

U(4) <sub>C</sub> × U(2) <sub>L</sub> × U(2) <sub>R</sub> × USp[2 <sup>2-β</sup> (4 - n <sub>g</sub> )] <sup>2</sup> × USp(2 <sup>2-β</sup> ) <sup>2</sup>												
	<i>N</i>	( <i>n</i> <sup>1</sup> , <i>l</i> <sup>1</sup> ) × ( <i>n</i> <sup>2</sup> , <i>l</i> <sup>2</sup> ) × ( <i>n</i> <sup>3</sup> , <i>l</i> <sup>3</sup> )	<i>n</i> <sub>S</sub>	<i>n</i> <sub>A</sub>	<i>b</i>	<i>b</i> '	<i>c</i>	<i>c</i> '	1	2	3	4
<i>a</i>	8	(0, -1) × (1, 1) × (1, 1)	0	0	2 <sup>1-β</sup> <i>n</i> <sub>g</sub>	0	-2 <sup>1-β</sup> <i>n</i> <sub>g</sub>	0	1	-1	0	0
<i>b</i>	4	( <i>n</i> <sub>g</sub> , 1) × (1, 0) × (1, -1)	2 <sup>1-β</sup> ( <i>n</i> <sub>g</sub> - 1)	-2 <sup>1-β</sup> ( <i>n</i> <sub>g</sub> - 1)	-	0	0	0	0	1	0	- <i>n</i> <sub>g</sub>
<i>c</i>	4	( <i>n</i> <sub>g</sub> , -1) × (0, 1) × (1, -1)	-2 <sup>1-β</sup> ( <i>n</i> <sub>g</sub> - 1)	2 <sup>1-β</sup> ( <i>n</i> <sub>g</sub> - 1)	-	-	-	0	-1	0	<i>n</i> <sub>g</sub>	0
1	2 <sup>2-β</sup> (4 - <i>n</i> <sub>g</sub> )	(1, 0) × (1, 0) × (2 <sup>β</sup> , 0)	$x_A = x_B = n_g \cdot x_C = n_g \cdot x_D \leftrightarrow \chi_1 = n_g, \chi_2 = 1, \chi_3 = 2^\beta$									
2	2 <sup>2-β</sup> (4 - <i>n</i> <sub>g</sub> )	(1, 0) × (0, -1) × (0, 2 <sup>β</sup> )	$\beta_1^g = -3, \beta_2^g = -3$									
3	2 <sup>2-β</sup>	(0, -1) × (1, 0) × (0, 2 <sup>β</sup> )	$\beta_3^g = -6 + n_g$									
4	2 <sup>2-β</sup>	(0, -1) × (0, 1) × (2 <sup>β</sup> , 0)	$\beta_4^g = -6 + n_g$									

where  $\phi_4 = \ln g_s$  is the four-dimensional dilaton. Inserting these expressions into Eq. (13), one finds that the gauge couplings are unified as  $g_s^2 = g_w^2 = \frac{5}{3}g_Y^2 = g^2$  at the string scale  $M_X$ ,

$$\frac{g^2(M_X)}{4\pi} = \left(\frac{2^\beta}{n_g}\right)^{1/2} e^{\phi_4}, \quad (18)$$

with the value of  $\phi_4$  fixed by the value of the gauge couplings where they unify,  $g^2(M_X)$ , which assumes different values for models with different numbers of generations at  $M_X = 2.2 \times 10^{16}$  GeV:

$$g^2|_{N_g=1}(M_X) = 0.275, \quad g^2|_{N_g=2}(M_X) = 0.358, \quad g^2|_{N_g=3}(M_X) = 0.511, \quad g^2|_{N_g=4}(M_X) = 0.895. \quad (19)$$

The corresponding string scale is then given by

$$M_{\text{St}} = \frac{g^2(M_X)}{4\pi} \left(\frac{n_g \pi}{2^\beta}\right)^{1/2} M_{\text{Planck}}, \quad (20)$$

where  $M_{\text{Planck}}$  is the reduced Planck scale,  $2.44 \times 10^{18}$  GeV.

After fixing the value of  $\phi_4$ , one can then determine the values of the gauge couplings for the hidden-sector gauge groups at the string scale:

$$g_{\text{USp}_j}^2 = 2^{(4-\beta/2)} \pi n_g^{(\rho_j/2)} e^{\phi_4}, \quad (21)$$

where  $\rho_1 = \rho_2 = +1$  and  $\rho_3 = \rho_4 = -1$ . Using the beta-function parameters  $\beta_j$  in Table 2, the scale at which each hidden-sector gauge group becomes confining can be calculated:

$$\Lambda_j = M_X \cdot \exp \left\{ \frac{2\pi}{-\beta_j} \left[ 1 - \frac{2^\beta \pi}{g^2(M_X) n_g^{(\rho_j+1)/2}} \right] \right\}. \quad (22)$$



Table 3: The chiral and vectorlike superfields of the model, and their quantum numbers under the gauge symmetry  $U(4)_C \times U(2)_L \times U(2)_R \times \text{USp}[2^{2-\beta}(4 - n_g)]^2 \times \text{USp}(2^{2-\beta})^2$ .

	Multiplicity	Quantum Number	$Q_4$	$Q_{2L}$	$Q_{2R}$	Field
$ab$	$2^{1-\beta}n_g$	$(4, \bar{2}, 1, 1, 1, 1, 1)$	1	-1	0	$F_L(Q_L, L_L)$
$ac$	$2^{1-\beta}n_g$	$(\bar{4}, 1, 2, 1, 1, 1, 1)$	-1	0	1	$F_R(Q_R, L_R)$
$a1$	1	$(4, 1, 1, \bar{N}_1, 1, 1, 1)$	1	0	0	$X_{a1}$
$a2$	1	$(\bar{4}, 1, 1, 1, N_2, 1, 1)$	-1	0	0	$X_{a2}$
$b2$	1	$(1, 2, 1, 1, \bar{N}_2, 1, 1)$	0	1	0	$X_{b2}$
$b4$	$n_g$	$(1, \bar{2}, 1, 1, 1, 1, N_4)$	0	-1	0	$X_{b4}^i$
$c1$	1	$(1, 1, \bar{2}, N_1, 1, 1, 1)$	0	0	-1	$X_{c1}$
$c3$	$n_g$	$(1, 1, 2, 1, 1, \bar{N}_3, 1)$	0	0	1	$X_{c3}^i$
$b_S$	$2^{1-\beta}(n_g - 1)$	$(1, 3, 1, 1, 1, 1, 1)$	0	2	0	$T_L^i$
$b_A$	$2^{1-\beta}(n_g - 1)$	$(1, \bar{1}, 1, 1, 1, 1, 1)$	0	-2	0	$S_L^i$
$c_S$	$2^{1-\beta}(n_g - 1)$	$(1, 1, \bar{3}, 1, 1, 1, 1)$	0	0	-2	$T_R^i$
$c_A$	$2^{1-\beta}(n_g - 1)$	$(1, 1, 1, 1, 1, 1, 1)$	0	0	2	$S_R^i$
$ab'$	$n_g$	$(4, 2, 1, 1, 1, 1, 1)$	1	1	0	
	$n_g$	$(\bar{4}, \bar{2}, 1, 1, 1, 1, 1)$	-1	-1	0	
$ac'$	$n_g$	$(4, 1, 2, 1, 1, 1, 1)$	1	0	1	$\Phi_i$
	$n_g$	$(\bar{4}, 1, \bar{2}, 1, 1, 1, 1)$	-1	0	-1	$\bar{\Phi}_i$
$bc$	$2n_g$	$(1, 2, \bar{2}, 1, 1, 1, 1)$	0	1	-1	$H_u^i, H_d^i$
	$2n_g$	$(1, \bar{2}, 2, 1, 1, 1, 1)$	0	-1	1	

It can then be checked that the hidden-sector gauge groups have sufficiently negative  $\beta_j$  to become confining at high-energy scales. To have only one pair of light Higgs doublets, as is necessary in the MSSM in order for the gauge couplings to unify, one must fine-tune the mixing parameters of the Higgs doublets, specifically by fine-tuning the  $\mu$  term in the superpotential. In particular, the  $\mu$  term and right-handed neutrino masses which may be generated via the higher-dimensional operators [48]:

$$W \supset \frac{y_\mu^{ijkl}}{M_{\text{St}}} S_L^i S_R^j H_u^k H_d^l + \frac{y_{N_{ij}^{mnkl}}}{M_{\text{St}}^3} T_R^m T_R^n \Phi_i \Phi_j F_R^k F_R^l, \quad (23)$$

where  $y_\mu^{ijkl}$  and  $y_{N_{ij}^{mnkl}}$  are Yukawa couplings, and  $M_{\text{St}}$  is the string scale. Thus, the  $\mu$  term is TeV scale and the right-handed neutrino masses can be in the range  $10^{10-14}$  GeV for  $y_\mu^{ijkl} \sim 1$  and  $y_{N_{ij}^{mnkl}} \sim 10^{(-7)-(-3)}$  where  $y_\mu^{ijkl}$  are Yukawa couplings,  $M_{\text{St}}$  is the string scale, and the singlets  $S_R^j$  and triplets  $T_R^j$  are assumed to receive string-scale VEVs, while the VEVs of the singlets  $S_L^i$  are TeV-scale. The exact linear combinations that give the two light Higgs eigenstates are correlated with the pattern of Higgs VEVs necessary to obtain Yukawa matrices for the quarks and leptons,

$$H_{u,d} = \sum_i \frac{v_{u,d}^i}{\sqrt{\sum (v_{u,d}^i)^2}}, \quad (24)$$

where  $v_{u,d}^i = \langle H_{u,d}^i \rangle$ . Thus, at low energies one obtains MSSM-like models with different numbers of generations, with gauge-coupling unification  $\sim 2.2 \times 10^{16}$  GeV, and matter charged under the hidden-sector gauge groups becomes confined into massive bound states at high-energy scales.

As has been , quantities such as gauge and Yukawa couplings depend on the VEVs of the closed-string moduli that parametrize the size and shape of the compactified manifold, as well as the open-string moduli that parametrize the positions of the D6-branes in the internal space, which are associated with the presence of three chiral adjoints in each stack. These VEVs should be determined dynamically. While it is not our goal to solve this problem in the present work, it should be mentioned that mechanisms do exist by which this can be accomplished. In particular, the closed-string moduli can be stabilized in AdS by turning on fluxes in Type IIA [60]. In fact, this mechanism has already been demonstrated for the three-generation model [61]. Also, gaugino condensation in the hidden sectors can provide another source of closed-string moduli stabilization [59]. The open-string moduli may be frozen if the D-branes wrap rigid cycles, a possibility that can exist on the  $T^6/(\mathbb{Z}_2 \times \mathbb{Z}_2)$  orientifold with discrete torsion [62, 63, 64]. An example of a four-generation MSSM-like model constructed from D6-branes wrapping rigid cycles is given in [37]. We emphasize the possibility of finding a dynamical reason to explain why nature chooses a specific number of chiral generations by studying the moduli stabilization problem for models with different numbers of generations, such as our mini-landscape of models.

### 3 Yukawa Couplings.

As one can see from the previous section (note the filler brane stacks in Table 3), only the models with  $n_g \leq 4$  can satisfy the tadpole conditions without introducing fluxes. If we take this condition as a constraint, then the only viable models from the top-down point of view have  $N_g = 1, 2, 3, 4, 6$ , and 8. Furthermore, masses may be generated via trilinear couplings for all generations only for those models with a tilted third torus ( $\beta = 1$ ). If we also take this condition as a constraint, then the only viable models are those with  $N_g = 1, 2, 3$ , and 4. Additionally, the  $SU(3)_C$  factor in the SM gauge group is only asymptotically free for SUSY models with four generations or less. Thus, the maximum viable number of generations is four.

The three-generation model has previously been studied in [48]. As mentioned in the Introduction, this model exhibits rank-3 Yukawa matrices and it is possible to nearly reproduce the correct masses and mixings for the three known generations of quarks and leptons. However, the Dirac mass matrix for neutrinos was not considered. Furthermore, there were difficulties obtaining the correct muon and electron masses which required additional corrections from four-point functions [65].

A complete form for the Yukawa couplings  $y_{ij}^f$  for D6-branes wrapping on a full compact space  $T^2 \times T^2 \times T^2$  can be expressed as [34, 47]:

$$Y_{\{ijk\}} = h_{qu} \sigma_{abc} \prod_{r=1}^3 \vartheta \left[ \begin{array}{c} \delta^{(r)} \\ \phi^{(r)} \end{array} \right] (\kappa^{(r)}), \quad (25)$$

where

$$\vartheta \left[ \begin{array}{c} \delta^{(r)} \\ \phi^{(r)} \end{array} \right] (\kappa^{(r)}) = \sum_{l \in \mathbf{Z}} e^{\pi i (\delta^{(r)} + l)^2 \kappa^{(r)}} e^{2\pi i (\delta^{(r)} + l) \phi^{(r)}}, \quad (26)$$

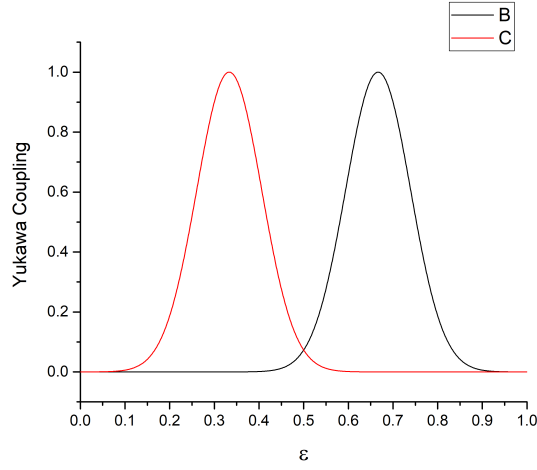


Figure 2: Yukawa couplings  $B$  and  $C$  as a function of shift parameter  $\epsilon$ . Here it may be seen that  $B = C$  for  $\epsilon = 0$  and  $\epsilon = 1/2$ .

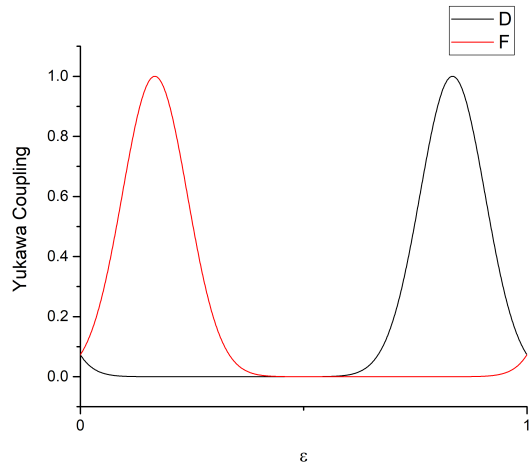


Figure 3: Yukawa couplings  $D$  and  $F$  as a function of shift parameter  $\epsilon$ . Here it may be seen that  $D = F$  for  $\epsilon = 0$  and  $\epsilon = 1/2$ .

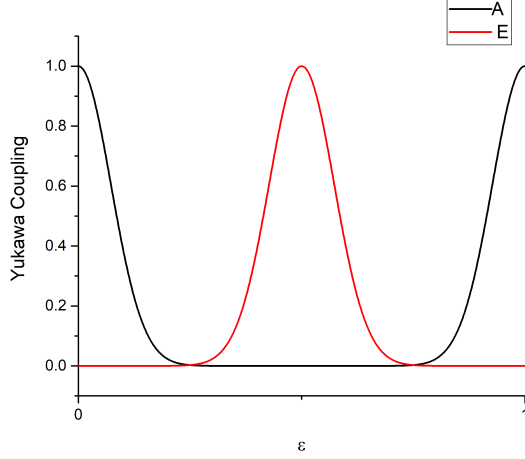


Figure 4: Yukawa couplings and  $A$  and  $E$  as a function of shift parameter  $\epsilon$ . Here it may be seen that  $A = 1$  and  $E = 0$  for  $\epsilon = 0$  and  $A = 0$  and  $E = 1$  for  $\epsilon = 1/2$ .

with  $r = 1, 2, 3$  denoting the three two-tori. The input parameters are given by

$$\begin{aligned}\delta^{(r)} &= \frac{i^{(r)}}{I_{ab}^{(r)}} + \frac{j^{(r)}}{I_{ca}^{(r)}} + \frac{k^{(r)}}{I_{bc}^{(r)}} + \frac{d^{(r)}(I_{ab}^{(r)}\epsilon_c^{(r)} + I_{ca}^{(r)}\epsilon_b^{(r)} + I_{bc}^{(r)}\epsilon_a^{(r)})}{I_{ab}^{(r)}I_{bc}^{(r)}I_{ca}^{(r)}} + \frac{s^{(r)}}{d^{(r)}}, \\ \phi^{(r)} &= \frac{I_{bc}^{(r)}\theta_a^{(r)} + I_{ca}^{(r)}\theta_b^{(r)} + I_{ab}^{(r)}\theta_c^{(r)}}{d^{(r)}}, \\ \kappa^{(r)} &= \frac{J^{(r)} |I_{ab}^{(r)}I_{bc}^{(r)}I_{ca}^{(r)}|}{\alpha' (d^{(r)})^2}.\end{aligned}\tag{27}$$

where the indices  $i^{(r)}$ ,  $j^{(r)}$ , and  $k^{(r)}$  label the intersections on the  $r^{\text{th}}$  torus,  $d^{(r)} = \gcd(I_{ab}^{(r)}, I_{bc}^{(r)}, I_{ca}^{(r)})$ , and the integer  $s^{(r)}$  is a function of  $i^{(r)}$ ,  $j^{(r)}$ , and  $k^{(r)}$  corresponding to different ways of counting triplets of intersections. The shift parameters  $\epsilon_a^{(r)}$ ,  $\epsilon_b^{(r)}$ , and  $\epsilon_c^{(r)}$  correspond to the relative positions of stacks  $a$ ,  $b$ , and  $c$ , while the parameters  $\theta_a^{(r)}$ ,  $\theta_b^{(r)}$ , and  $\theta_c^{(r)}$  are Wilson lines associated with these stacks. For simplicity, we set the Wilson lines to zero. We also define the total shift parameter  $\epsilon$  to be

$$\epsilon = \frac{I_{ab}\epsilon_c + I_{ca}\epsilon_b + I_{bc}\epsilon_a}{I_{ab}I_{bc}I_{ca}},\tag{28}$$

so after comparing the parameters, we have

$$\delta = \frac{i}{I_{ab}} + \frac{j}{I_{ca}} + \frac{k}{I_{bc}} + \epsilon,\tag{29}$$

$$\phi = 0,\tag{30}$$

$$\kappa = \frac{J^{(r)} |I_{ab}^{(r)}I_{bc}^{(r)}I_{ca}^{(r)}|}{\alpha' (d^{(r)})^2}.\tag{31}$$

We focus only on the first torus, as the Yukawa couplings from the second and third tori only produce an overall constant. We label the left-handed fields, right-handed fields, and Higgs fields with the indices  $i$ ,  $j$ , and  $k$  respectively, which may assume the values

$$i \in \{0, 1, 2\}, \quad j \in \{0, 1, 2\}, \quad k \in \{0, 1, 2, 3, 4, 5\}.\tag{32}$$

A trilinear Yukawa coupling occurs for a given set of indices that satisfy the selection rule

$$i + j + k = 0 \pmod{3}. \quad (33)$$

By choosing a different linear function for  $s^{(1)}$ , some independent modes with non-zero eigenvalues are possible. Specifically, we will consider the case  $s^{(1)} = -i$ . This results in Yukawa matrices of the form

$$\mathcal{M} \sim \begin{pmatrix} Av_1 & Bv_3 & Cv_5 \\ Cv_3 & Av_5 & Bv_1 \\ Bv_5 & Cv_1 & Av_3 \end{pmatrix} + \begin{pmatrix} Ev_4 & Fv_6 & Dv_2 \\ Dv_6 & Ev_2 & Fv_4 \\ Fv_2 & Dv_4 & Ev_6 \end{pmatrix}, \quad (34)$$

where  $v_k = \langle H_{k+1} \rangle$  and the Yukawa couplings  $A, B, C, D, E$ , and  $F$  are given by

$$\begin{aligned} A &\equiv \vartheta \begin{bmatrix} \epsilon^{(1)} \\ \phi^{(1)} \end{bmatrix} \left( \frac{6J^{(1)}}{\alpha'} \right), & B &\equiv \vartheta \begin{bmatrix} \epsilon^{(1)} + \frac{1}{3} \\ \phi^{(1)} \end{bmatrix} \left( \frac{6J^{(1)}}{\alpha'} \right), \\ C &\equiv \vartheta \begin{bmatrix} \epsilon^{(1)} - \frac{1}{3} \\ \phi^{(1)} \end{bmatrix} \left( \frac{6J^{(1)}}{\alpha'} \right), & D &\equiv \vartheta \begin{bmatrix} \epsilon^{(1)} + \frac{1}{6} \\ \phi^{(1)} \end{bmatrix} \left( \frac{6J^{(1)}}{\alpha'} \right), \\ E &\equiv \vartheta \begin{bmatrix} \epsilon^{(1)} + \frac{1}{2} \\ \phi^{(1)} \end{bmatrix} \left( \frac{6J^{(1)}}{\alpha'} \right), & F &\equiv \vartheta \begin{bmatrix} \epsilon^{(1)} - \frac{1}{6} \\ \phi^{(1)} \end{bmatrix} \left( \frac{6J^{(1)}}{\alpha'} \right). \end{aligned} \quad (35)$$

These Yukawa matrices are of rank 3, which means that it is possible to have three different mass eigenvalues as well as mixing between each of the different generations. For certain values of the shift parameter  $\epsilon$ , namely  $\epsilon^{(1)} = 0 \pmod{0.5}$ , we find that some of the Yukawa couplings are equal due to the symmetry properties of the Jacobi Theta functions, Eq. (26). Specifically, we have that  $B = C$  and  $D = F$  at both  $\epsilon = 0$  and  $\epsilon = 1/2$  as may be seen in Figs. 2 and 3. Furthermore, at  $\epsilon = 0$  we find that  $A = 1$  while  $E = 0$ , and that at  $\epsilon = 1/2$  we have  $A = 1$  while  $E = 0$  as shown in Fig. 4

Let us observe that when the shift parameters take the values  $\epsilon^{(1)} = 0$  and  $\epsilon^{(1)} = 1/2$ , each of these mass matrices of the same form Eq. (5) as given by Ma [16], which results from a  $\Delta(27)$  flavor symmetry. This is due to the symmetry properties of the Jacobi Theta functions and the selection rule Eq. (33). In addition,  $\Delta(27)$  contains  $A_4$  as a subgroup so that it is also possible for a mass matrix of this form to give rise to near-tribimaximal mixing.

It should be noted that this matrix may be written as the sum of two matrices, one of which involves the odd-numbered Higgs VEVs and one involves the even-numbered Higgs VEVs, each of which may lead to near-tribimaximal mixing. We shall find this useful in the next section as the mass matrices for the up-type quarks and neutrinos must involve the same set of Higgs VEVs  $v_i^U$ , and the mass matrices for down-type quarks and charged leptons involves a different set of Higgs VEVs,  $v_i^D$ . In particular, we will find that the up and down-type quarks predominantly receive masses via the odd-numbered Higgs VEVs  $v_{\text{odd}}^{U,D}$  while the neutrinos and charged leptons obtain mass via the even-numbered Higgs VEVs  $v_{\text{even}}^{U,D}$  if the shift parameter is  $\epsilon^{(1)} = 0$  for the quarks and  $\epsilon^{(1)} = 1/2$  for the leptons respectively. Finally, in order to have a consistent solution, the following constraint must be satisfied

$$\epsilon_u + \epsilon_l = \epsilon_d + \epsilon_\nu, \quad (36)$$

in order to have a consistent solution.

## 4 Numerical Analysis.

The Yukawa couplings for the quarks and leptons are given by the superpotential

$$W_Y = Y_{ijk}^U Q_L^i U_R^j H_U^k + Y_{ijk}^D Q_L^i D_R^j H_D^k + Y_{ijk}^\nu L^i N^j H_U^k + Y_{ijk}^L L^i E^j H_D^k, \quad (37)$$

where the Yukawa couplings  $Y_{ijk}$  are given by Eq. (25) and have the general form given by Eq. (34).

We may determine the desired mass matrices for quarks and leptons by running the RGE's up to the unification scale, which is taken to be the string scale in the present context. For example, for  $\tan\beta \approx 50$  at the unification scale  $\mu = M_X$  the diagonal quark mass matrices  $D_u U_L^u M_u U_R^{u\dagger}$  and  $D_d = U_L^d M_d U_R^{d\dagger}$  may be determined to be [66, 67]

$$D_u = m_t \begin{pmatrix} 0.0000139 & 0 & 0 \\ 0 & 0.00404 & 0 \\ 0 & 0 & 1 \end{pmatrix}, \quad D_d = m_b \begin{pmatrix} 0.00141 & 0 & 0 \\ 0 & 0.0280 & 0 \\ 0 & 0 & 1 \end{pmatrix}, \quad (38)$$

with

$$V_{CKM} = U_L^d U_L^{u\dagger} = \begin{pmatrix} 0.9754 & 0.2205 & -0.0026i \\ -0.2203e^{0.003^\circ i} & 0.9749 & 0.0318 \\ 0.0075e^{-19^\circ i} & -0.0311e^{1.0^\circ i} & 0.9995 \end{pmatrix}, \quad (39)$$

where  $U^i$  are unitary diagonalization matrices. Similarly, the diagonal charged lepton mass matrix is given by

$$D_l = U_L^l M_l U_R^{l\dagger} = m_\tau \begin{pmatrix} 0.000217 & 0 & 0 \\ 0 & 0.0458 & 0 \\ 0 & 0 & 1 \end{pmatrix}. \quad (40)$$

For the Dirac mass matrix for the neutrinos, we desire that it has the form given in Eq. (5) so that its diagonalization matrix will be near-tribimaximal.

In order to fit the mass matrices  $M_u$ ,  $M_d$ , and  $M_l$ , we make specific choices for the set of Higgs VEVs  $v_k^{U,D}$  as well as the shift parameter for each stack of D-branes,  $\epsilon^{(1)}$ . In making choices for these parameters, it is useful to note that the Higgs VEVs with odd values of  $k$  may dominate the mass matrix when the shift parameter  $\epsilon^{(1)} = 0$ , while those with even values may dominate for  $\epsilon^{(1)} = 1/2$ . This is particularly true for large values of  $\kappa$ , and essentially results from the symmetry properties of the Jacobi Theta functions. For example, when  $\epsilon^{(1)} = 0$ , the Yukawa coupling  $A = 1$  while  $E = 0$ , but for  $\epsilon^{(1)} = 1/2$  this is reversed,  $A = 0$  while  $E = 1$  while the other Yukawa couplings  $B, C, D$ , and  $F$  tend to be smaller. This suggest that the odd Higgs VEVs  $v_{k=odd}^U$  primarily give mass to the up-type quarks, while the even Higgs VEVs  $v_{k=even}^U$  are responsible for the Dirac mass matrix for the neutrinos, provided we choose  $\epsilon_u^{(1)} = 0$  and  $\epsilon_\nu^{(1)} = 1/2$ . Similarly, the odd Higgs VEVs  $v_{k=odd}^D$  primarily give mass to the down-type quarks, while the even Higgs VEVs  $v_{k=even}^D$  are responsible for the charged lepton mass matrix, provided we choose  $\epsilon_d^{(1)} = 0$  and  $\epsilon_l^{(1)} = 1/2$ . In order to have a consistent solution, we also require that the shift parameters for each stack of D-branes satisfies the constraint

$$\epsilon_u^{(1)} + \epsilon_l^{(1)} = \epsilon_d^{(1)} + \epsilon_\nu^{(1)}, \quad (41)$$

which the above choices clearly satisfy.

## 4.1 Quark Masses and CKM Matrix

Thus, let us make the choices  $\kappa = 58.7$  and

$$\begin{aligned}
v_u^1 &= 0.0000142, & v_d^1 &= 0.0028224 \\
v_u^2 &= 0.00002408185, & v_d^2 &= 0.045 \\
v_u^3 &= 1.0, & v_d^3 &= 1.0 \\
v_u^4 &= 0.000000345, & v_d^4 &= 0.0010105 \\
v_u^5 &= 0.00404, & v_d^5 &= 0.0266 \\
v_u^6 &= 0.005960855, & v_d^6 &= 1.0.
\end{aligned} \tag{42}$$

In addition, let us set the shift parameters for the quarks to be  $\epsilon_u^{(1)} = \epsilon_d^{(1)} = 0$ . Note that the Higgs VEVs  $v_u^{even}$  have been chosen so that the neutrino mass matrix will be near-tribimaximal. We set all  $CP$  phases to zero. With these parameters, we obtain the following mass matrices for the up and down-type quarks:

$$M_u = m_t \begin{pmatrix} 0.0000142 & 0.00003553304 & 0.0000001436 \\ 0.00003553304 & 0.00404 & 0.000000002055 \\ 0.0000001436 & 0.000000002055 & 1 \end{pmatrix}, \tag{43}$$

$$M_d = m_b \begin{pmatrix} 0.0028224 & 0.005960856 & 0.0002682385 \\ 0.005960856 & 0.0266 & 0.000006023448 \\ 0.0002682385 & 0.000006023448 & 1 \end{pmatrix}. \tag{44}$$

The eigenavlues for these matrices are exactly those given by Eq. (38), while the diagonalization matrices for the up and down-type quarks are given by

$$U_L^u = \begin{pmatrix} 0.999961 & 0.008825 & 0.0 \\ -0.008825 & 0.999961 & 0.0 \\ 0.0 & 0.0 & 1 \end{pmatrix}, \tag{45}$$

$$U_L^d = \begin{pmatrix} 0.973122 & 0.230291 & 0.000269 \\ -0.023091 & 0.973122 & 0.000008 \\ -0.000268260 & -0.000070 & 1 \end{pmatrix}. \tag{46}$$

Then the CKM matrix is given by

$$V_{CKM} = U_L^d U_L^{u\dagger} = \begin{pmatrix} 0.9751 & 0.2217 & 0.003 \\ -0.2217 & 0.9751 & 0.0 \\ -0.0003 & -0.0001 & 1.0 \end{pmatrix}, \tag{47}$$

which is very close to the desired CKM matrix Eq. (39), though not exact.

## 4.2 Lepton Masses and PMNS Matrix

Let us set the shift parameters for the leptons to be  $\epsilon_\nu^{(1)} = \epsilon_l^{(1)} = 1/2$ . Then, using the same set of Higgs VEVs as before, we obtain mass matrices for the neutrinos and charged leptons given by

$$M_\nu = m_t \begin{pmatrix} 0.000000345 & 0.005960855 & 0.00002408185 \\ 0.005960855 & 0.00002408185 & 0.00000008464414 \\ 0.00002408185 & 0.00000008464414 & 0.005960855 \end{pmatrix}, \tag{48}$$

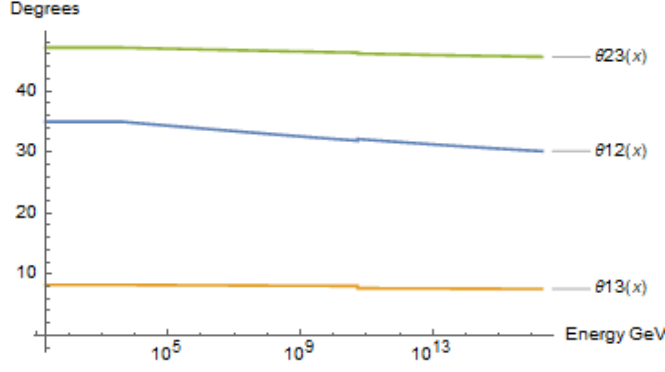


Figure 5: Neutrino mixing angles as a function of energy scale.

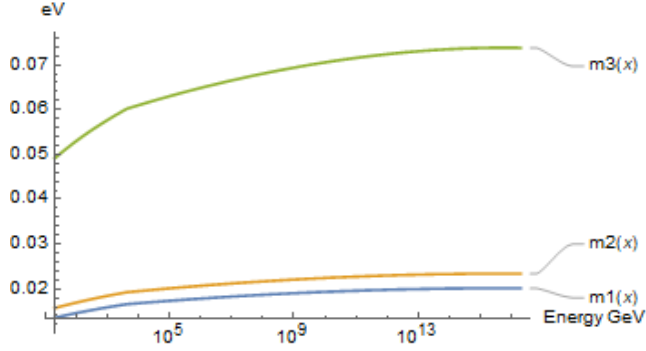


Figure 6: Neutrino masses as a function of energy scale. Note that we have taken the supersymmetry decoupling scale to be 4.28 TeV in order to obtain the best agreement with data.

$$M_l = m_b \begin{pmatrix} 0.0010105 & 0.005960856 & 0.0001585588 \\ 0.005960856 & 0.045 & 0.00001682392 \\ 0.0001585588 & 0.00001682392 & 1 \end{pmatrix}. \quad (49)$$

The eigenvalues for the charged lepton mass matrix are exactly those given by Eq. (40), assuming that  $m_\tau = m_b$ . Thus, we find that it is possible to accommodate the correct masses for quarks and charged leptons, as well as nearly the correct CKM matrix for quarks.

The diagonalization matrices for the Dirac neutrinos and charged leptons are given by

$$U_L^\nu = \begin{pmatrix} 0.707811 & 0.578043 & -0.406042 \\ -0.706400 & 0.578034 & -0.408504 \\ -0.001426 & 0.575972 & 0.817468 \end{pmatrix}, \quad (50)$$

$$U_L^l = \begin{pmatrix} 0.991257 & 0.131942 & 0.000159 \\ -0.131942 & 0.9912157 & 0.000019 \\ -0.000155 & -0.000039 & 1 \end{pmatrix}. \quad (51)$$

Here, we can see that the Dirac neutrino mass matrix is near-tribimaximal while the charged lepton mass matrix is near-diagonal. Of course, to explain the observed tiny neutrino masses, usually the Dirac neutrino mass matrix is input into a seesaw mechanism to produce a resulting Majorana mass matrix. In order for the canonical seesaw mechanism to work, there must exist a mass term for right-handed neutrinos in the superpotential. As discussed previously such a



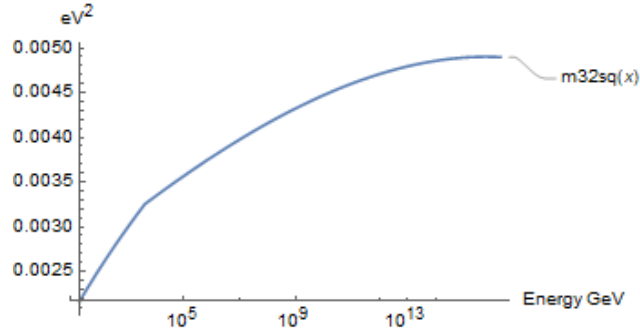


Figure 7: Mass difference  $m_{32}^2$  as a function of energy scale. Note that we have taken the supersymmetry decoupling scale to be 4.28 TeV in order to obtain the best agreement with data.

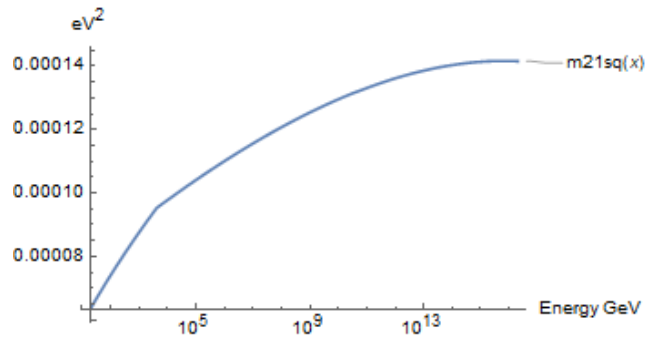


Figure 8: Mass difference  $m_{21}^2$  as a function of energy scale. Note that we have taken the supersymmetry decoupling scale to be 4.28 TeV in order to obtain the best agreement with data.

term is present in the model, *viz* Eq. (23). However, this term is of very high order, and it is not currently possible to calculate. In principle, such couplings may be induced by D-brane instantons [49, 50, 51]. However, this is not possible in the present model since the right-handed neutrino fields are charged under a gauged  $U(1)_{B-L}$ .

In order to calculate Majorana masses for the neutrinos, we need to make some assumptions regarding the right-handed neutrino masses. Let us observe that for the near tribimaximal mixing to be preserved after the seesaw mechanism is applied, the right-handed neutrino masses need to be nearly degenerate. Thus, let us make the choice

$$M_R^{-1} = -\frac{1}{M_r} \begin{pmatrix} 0.9990 & 0 & 0 \\ 0 & 0.99939 & 0 \\ 0 & 0 & 1 \end{pmatrix}. \quad (52)$$

where  $M_r \sim 10^{10}$  GeV. for the inverse right-handed neutrino mass matrix. Then, applying the canonical seesaw mechanism,

$$M_\nu^M = -M_\nu M_R^{-1} M_\nu^T, \quad (53)$$

we find that the Majorana neutrino mass matrix is given by

$$M_M^\nu = \begin{pmatrix} 3.5513 & 0.01460 & 0.0144 \\ 0.0146 & 3.5497 & 0.0144 \\ 0.0144 & 0.0144 & 3.5532 \end{pmatrix} \cdot 10^{-3}, \quad (54)$$

The diagonalization matrix for the Majorana neutrino mass matrix remains near-tribimaximal,

$$U_M^\nu = \begin{pmatrix} 0.6086 & 0.5482 & 0.5737 \\ -0.7808 & 0.2851 & 0.5559 \\ 0.1412 & -0.7863 & -0.6015 \end{pmatrix}, \quad (55)$$

In addition, the mass eigenvalues are given by

$$m_1 = 3.5357 m_\nu, \quad m_2 = 3.5380 m_\nu, \quad m_3 = 3.5803 m_\nu, \quad (56)$$

which is normal-ordered. If we chose  $m_\nu = 0.1$  eV, we find that the differences in the mass-squared values are

$$\Delta m_{32}^2 = 0.003 \text{ eV}^2, \quad \Delta m_{21}^2 = 0.000163 \text{ eV}^2 \quad (57)$$

which are comparable with the results of oscillation experiments [1, 5]. However, these results seem to be inconsistent with limits on the sum of neutrino masses from cosmological data [9, 10, 11].

$$\sum_i \nu_i \lesssim 0.12 \text{ eV}. \quad (58)$$

On the other hand, it should be remembered that these are the masses at the string scale, rather than at low energy where the experiments are performed. The RGE running of these masses could change these results, although the change is not expected to be large. The RGE running of the neutrino mass parameters in the MSSM with  $\tan \beta = 50$  has been studied in [68].

The lepton mixing matrix is given by

$$V_{PMNS} = U_L^{\dagger} U_M^{\nu} = \begin{pmatrix} 0.7063 & 0.5059 & 0.4952 \\ -0.6891 & 0.3590 & -0.6310 \\ 0.1413 & -0.7862 & -0.6016 \end{pmatrix}, \quad (59)$$

which may be reordered as

$$V_{PMNS} = \begin{pmatrix} 0.7862 & -0.6016 & 0.1413 \\ 0.3590 & -0.6310 & -0.6891 \\ 0.5059 & 0.4952 & 0.7063 \end{pmatrix}. \quad (60)$$

This result may compared to the  $3\sigma$  ranges on the PMNS matrix [2]:

$$|V|_{PMNS}^{3\sigma} = \begin{pmatrix} 0.797 \rightarrow 0.842 & 0.518 \rightarrow 0.585 & 0.143 \rightarrow 0.156 \\ 0.233 \rightarrow 0.495 & 0.448 \rightarrow 0.679 & 0.639 \rightarrow 0.783 \\ 0.287 \rightarrow 0.532 & 0.486 \rightarrow 0.706 & 0.604 \rightarrow 0.754 \end{pmatrix}. \quad (61)$$

It may be observed that the absolute values of the PMNS matrix elements obtained in the model agree relatively well with the experimentally observed values. However, once again it should be kept in mind that the obtained PMNS matrix is calculated at the string scale, while the experimentally obtained mixing angles are obtained at low energy. Thus, one should consider the RGE running of these parameters when making a true comparison. This may be performed in the REAP Mathematica package [69], taking the above Yukawa matrices for quarks and leptons as input. As will be discussed in detail in [70], if we chose the right-handed neutrino mass matrix to be

$$M_R = M_r \cdot \begin{pmatrix} -5.15192 & -0.279985 & 0.249735 \\ -0.279985 & -3.13943 & 1.7322 \\ 0.249735 & 1.7322 & 3.15014 \end{pmatrix} \quad (62)$$

and start the RGE running from the conventional GUT scale  $M_{GUT} = 2 \cdot 10^{16}$  GeV down to the electroweak scale, we obtain mixing angles which are consistent with current observations

$$\theta_{12} = 35.0^\circ, \quad \theta_{12} = 47.1^\circ, \quad \theta_{13} = 8.27^\circ. \quad (63)$$

A plot of the neutrino mixing angles as a function of energy scale is shown in Fig. 5. In addition, we find that the neutrino masses are given by

$$m_1 = 0.0146 \text{ eV}, \quad m_2 = 0.0170 \text{ eV}, \quad m_3 = 0.0530 \text{ eV}, \quad (64)$$

with

$$\Delta m_{32}^2 = 0.00252 \text{ eV}^2, \quad \Delta m_{21}^2 = 0.00000739 \text{ eV}^2. \quad (65)$$

These values are consistent with current experimental observations as well as constraints on the sum of neutrino masses from cosmological data. A plot of the neutrino masses as a function of energy scale is shown in Fig. 6. In addition, plots of  $m_{32}^2$  and  $m_{21}^2$  as functions of energy scale are shown in Fig. 7 and Fig. 8. Note that we have taken the supersymmetry decoupling scale to be 4.28 TeV in order to obtain the best agreement with data. It would also be interesting to study the RGE running including light vector-like states as it has been shown previously that such states may exist in this model in complete  $SU(5)$  multiplets [71]. We save this for future work.

## 5 Conclusion.

We have studied the Yukawa mass matrices in a realistic MSSM constructed with intersecting D6 branes on a  $T^6/(\mathbb{Z}_2 \times \mathbb{Z}_2)$  orientifold. It has been shown that correct mass matrices for quarks and charged leptons may be obtained in the model. Though a similar result has been demonstrated in previous work, before to obtain the correct masses for the muon and electron required additional corrections from four-point functions. Here, they are obtained with only trilinear couplings. In addition, we have obtained a CKM quark mixing matrix which is nearly correct.

Moreover, we have also shown that the generic Dirac mass matrices in the model are of the same form as those shown by Ma to lead to near-tribimaximal mixing. We have shown that this occurs naturally in the model. Though tribimaximal mixing has been ruled out by experiments, it still may be used as a zeroth order approximation. Thus, we calculate a Dirac mass matrix which is consistent with the obtained mass matrices for quarks and leptons. In order to preserve the near-tribimaximal mixing after the seesaw mechanism, we assumed that the right-handed neutrino masses are nearly degenerate. Whether or not this assumption is justified will require the detailed calculation of the right-handed neutrino mass matrix.

After the seesaw mechanism, we obtained a Majorana neutrino mass matrix with mass eigenvalues that are such that the differences in the mass-squared values between neutrino masses may almost be obtained. However, the sum of the neutrino mass eigenvalues is not consistent with the constraints from cosmological data by roughly a factor of three. Finally a PMNS lepton mixing matrix is obtained with elements which are mostly consistent with the experimentally observed values. It should be pointed out that this result is dependent on small differences between the right-handed neutrino masses, as well as corrections from the charged lepton sector.

We also discussed that the calculated values for the neutrino masses and PMNS matrix elements are at the string scale, whereas the experimentally observed values are at low-energies. We performed an RGE analysis of the neutrino mass parameters, including the seesaw mechanism assuming a specific form for the right-handed neutrino mass matrix, and found that the neutrino mixing angles at the electroweak scale are consistent with experimental data. Specifically, we found that  $\theta_{12} = 35.0^\circ$ ,  $\theta_{23} = 47.1^\circ$ , and  $\theta_{13} = 8.27^\circ$ . In addition, we found the neutrino mass-squared differences to be  $\Delta m_{32}^2 = 0.00252 \text{ eV}^2$  and  $\Delta m_{21}^2 = 0.0000739 \text{ eV}^2$  with  $m_1 = 0.0146 \text{ eV}$ ,  $m_2 = 0.0170 \text{ eV}$ , and  $m_3 = 0.0530 \text{ eV}$ . These results depend slightly upon the scale at which the RGE running goes from being that of the MSSM to that of the SM, which we interpret to be the lightest stop mass. The best agreement with experimental data is for  $\tilde{m}_{t_1} \approx 4.28 \text{ TeV}$ . This suggests that the superpartners which produce the strongest signal in a hadron collider are just out of reach at the LHC.

Our approach here has been to take the known quark masses, CKM matrix, charged lepton masses, and the requirement for near-tribimaximal mixing for the neutrinos as input which are then fitted in the model to fix model parameters. This was then used to determine the Dirac mass matrix for the neutrinos which is consistent with this fit. We then performed an RGE analysis of the neutrino mass parameters, which allows a prediction for the neutrino masses to be made. Of course, the main weakness of this approach at the moment is in the right-handed neutrino mass matrix, which is treated as a free parameter in this analysis. However, in principle even this may be calculated from the model. We plan to focus on this in future work.

**Acknowledgements.** I would like to thank my students Evan Howington, Jordan Gemmill, and Matt Teel for useful discussions during early parts of this work.

## References

- [1] T. Araki *et al.* [KamLAND Collaboration], Phys. Rev. Lett. **94**, 081801 (2005) doi:10.1103/PhysRevLett.94.081801 [hep-ex/0406035].
- [2] I. Esteban, M. C. Gonzalez-Garcia, A. Hernandez-Cabezudo, M. Maltoni and T. Schwetz, arXiv:1811.05487 [hep-ph].
- [3] I. Esteban, M. C. Gonzalez-Garcia, M. Maltoni, I. Martinez-Soler and T. Schwetz, JHEP **1701**, 087 (2017) doi:10.1007/JHEP01(2017)087 [arXiv:1611.01514 [hep-ph]].
- [4] NuFit, <http://www.nu-fit.org/>
- [5] Y. Fukuda *et al.* [Super-Kamiokande Collaboration], Phys. Rev. Lett. **81**, 1158 (1998) Erratum: [Phys. Rev. Lett. **81**, 4279 (1998)] doi:10.1103/PhysRevLett.81.1158, 10.1103/PhysRevLett.81.4279 [hep-ex/9805021].
- [6] S. Vagnozzi, E. Giusarma, O. Mena, K. Freese, M. Gerbino, S. Ho and M. Lattanzi, Phys. Rev. D **96**, no. 12, 123503 (2017) doi:10.1103/PhysRevD.96.123503 [arXiv:1701.08172 [astro-ph.CO]].
- [7] E. Giusarma, M. Gerbino, O. Mena, S. Vagnozzi, S. Ho and K. Freese, Phys. Rev. D **94**, no. 8, 083522 (2016) doi:10.1103/PhysRevD.94.083522 [arXiv:1605.04320 [astro-ph.CO]].
- [8] E. Giusarma, S. Vagnozzi, S. Ho, S. Ferraro, K. Freese, R. Kamen-Rubio and K. B. Luk, Phys. Rev. D **98**, no. 12, 123526 (2018) doi:10.1103/PhysRevD.98.123526 [arXiv:1802.08694 [astro-ph.CO]].
- [9] S. A. Thomas, F. B. Abdalla and O. Lahav, Phys. Rev. Lett. **105**, 031301 (2010) doi:10.1103/PhysRevLett.105.031301 [arXiv:0911.5291 [astro-ph.CO]].
- [10] P. A. R. Ade *et al.* [Planck Collaboration], Astron. Astrophys. **571**, A16 (2014) doi:10.1051/0004-6361/201321591 [arXiv:1303.5076 [astro-ph.CO]].
- [11] R. A. Battye and A. Moss, Phys. Rev. Lett. **112**, no. 5, 051303 (2014) doi:10.1103/PhysRevLett.112.051303 [arXiv:1308.5870 [astro-ph.CO]].
- [12] F. P. An *et al.* [Daya Bay Collaboration], Phys. Rev. Lett. **108**, 171803 (2012) doi:10.1103/PhysRevLett.108.171803 [arXiv:1203.1669 [hep-ex]].
- [13] Y. Abe *et al.* [Double Chooz Collaboration], Phys. Rev. Lett. **108**, 131801 (2012) doi:10.1103/PhysRevLett.108.131801 [arXiv:1112.6353 [hep-ex]].
- [14] J. K. Ahn *et al.* [RENO Collaboration], Phys. Rev. Lett. **108**, 191802 (2012) doi:10.1103/PhysRevLett.108.191802 [arXiv:1204.0626 [hep-ex]].
- [15] E. Ma, Phys. Rev. D **73**, 057304 (2006) doi:10.1103/PhysRevD.73.057304 [hep-ph/0511133].
- [16] E. Ma, Phys. Lett. B **660**, 505 (2008) doi:10.1016/j.physletb.2007.12.060 [arXiv:0709.0507 [hep-ph]].

- [17] A.M. Uranga, *Class. Quant. Grav.* 20 (2003) S373.
- [18] R. Blumenhagen, M. Cvetič, P. Langacker, G. Shiu, *Ann. Rev. Nucl. Part. Sci.* 55 (2005) 71.
- [19] R. Blumenhagen, B. Körs, D. Lüst, S. Stieberger, *Phys. Rept.* 445 (2007) 1.
- [20] F. Marchesano, *Fortsch. Phys.* 55 (2007) 491.
- [21] M.R. Douglas, G. Moore, *D-branes, quivers and ALE instantons*, hep-th/9603167.
- [22] M. Berkooz, M.R. Douglas, R.G. Leigh, *Nucl. Phys. B* 480 (1996) 265.
- [23] G. Aldazabal, S. Franco, L.E. Ibáñez, R. Rabadán, A.M. Uranga, *J. Math. Phys.* 42 (2001) 3103; *J. High Ener. Phys.* 0102 (2001) 047.
- [24] C. Bachas, *A Way to break supersymmetry*, hep-th/9503030.
- [25] R. Blumenhagen, L. Görlich, B. Körs, D. Lüst, *J. High Ener. Phys.* 0010 (2000) 006; R. Blumenhagen, B. Körs, D. Lüst, *J. High Ener. Phys.* 0102 (2001) 030.
- [26] C. Angelantonj, I. Antoniadis, E. Dudas, A. Sagnotti, *Phys. Lett. B* 489 (2000) 223.
- [27] D. Cremades, L.E. Ibáñez, F. Marchesano, *J. High Ener. Phys.* 0207 (2002) 009.
- [28] M. Cvetič, G. Shiu, A.M. Uranga, *Nucl. Phys. B* 615 (2001) 3.
- [29] M. Cvetič, G. Shiu, A.M. Uranga, *Phys. Rev. Lett.* 87 (2001) 201801; *Nucl. Phys. B* 615 (2001) 3.
- [30] J.C. Pati, A. Salam, *Phys. Rev. D* 8 (1973) 1240.
- [31] H. Georgi, S.L. Glashow, *Phys. Rev. Lett.* 32 (1974) 438.
- [32] G. K. Leontaris and J. Rizos, *Phys. Lett. B* **510**, 295 (2001) doi:10.1016/S0370-2693(01)00592-5 [hep-ph/0012255].
- [33] P. Anastasopoulos, G. K. Leontaris and N. D. Vlachos, *JHEP* **1005**, 011 (2010) doi:10.1007/JHEP05(2010)011 [arXiv:1002.2937 [hep-th]].
- [34] M. Cvetič, I. Papadimitriou, *Phys. Rev. D* 67 (2003) 126006; M. Cvetič, T. Li, T. Liu, *Nucl. Phys. B* 698 (2004) 163.
- [35] M. Cvetič, I. Papadimitriou, G. Shiu, *Nucl. Phys. B* 659 (2003) 193; (E) *Nucl. Phys. B* 696 (2004) 298.
- [36] M. Cvetič, P. Langacker, T. Li, T. Liu, *Nucl. Phys. B* 709 (2005) 241.
- [37] C.M. Chen, T. Li, D.V. Nanopoulos, *Nucl. Phys. B* 740 (2006) 79.
- [38] I. Antoniadis and G. K. Leontaris, *Phys. Lett. B* **216**, 333 (1989). doi:10.1016/0370-2693(89)91125-8

- [39] I. Antoniadis, G. K. Leontaris and J. Rizos, Phys. Lett. B **245**, 161 (1990). doi:10.1016/0370-2693(90)90127-R
- [40] R. Blumenhagen, F. Gmeiner, G. Honecker, D. Lüüst, T. Weigand, Nucl. Phys. B 713 (2005) 83.
- [41] F. Gmeiner, R. Blumenhagen, G. Honecker, D. Lüüst, T. Weigand, J. High Ener. Phys. 0601 (2006) 004.
- [42] G. Honecker, T. Ott, Phys. Rev. D 70 (2004) 126010; (E) Phys. Rev. D 71 (2005) 069902.
- [43] S.M. Barr, Phys. Rev. D 40 (1989) 2457;  
J.P. Derendinger, J.E. Kim, D.V. Nanopoulos, Phys. Lett. B 139 (1984) 170;  
I. Antoniadis, J.R. Ellis, J.S. Hagelin, D.V. Nanopoulos, Phys. Lett. B 194 (1987) 231.
- [44] J.R. Ellis, P. Kanti, D.V. Nanopoulos, Nucl. Phys. B 647 (2002) 235;  
C.M. Chen, G.V. Kraniotis, V.E. Mayes, D.V. Nanopoulos, J.W. Walker, Phys. Lett. B 611 (2005) 156; (E) Phys. Lett. B 625 (2005) 96;  
C.M. Chen, V.E. Mayes, D.V. Nanopoulos, Phys. Lett. B 633 (2006) 618;  
C.M. Chen, T. Li, D.V. Nanopoulos, Nucl. Phys. B 751 (2006) 260.
- [45] M. Axenides, E. Floratos, C. Kokorelis, J. High Ener. Phys. 0310 (2003) 006.
- [46] H. Abe, K.S. Choi, T. Kobayashi, H. Ohki, Nucl. Phys. B 820 (2009) 317. J. High Ener. Phys. 0901 (2009) 059.
- [47] D. Cremades, L.E. Ibáñez, F. Marchesano, *Towards a theory of quark masses, mixings and CP-violation*, arXiv:hep-ph/0212064; J. High Ener. Phys. 0307 (2003) 038.
- [48] C.M. Chen, T. Li, V.E. Mayes, D.V. Nanopoulos, Phys. Lett. B 665 (2008) 267;
- [49] S.A. Abel, M.D. Goodsell, J. High Ener. Phys. 0710 (2007) 034.
- [50] M. Cvetič, J. Halverson, R. Richter, J. High Ener. Phys. 0912 (2009) 063.
- [51] M. Cvetič, J. Halverson, R. Richter, J. High Ener. Phys. 1007 (2010) 005. Phys. Rev. D 77 (2008) 125023.
- [52] E.G. Gimon, J. Polchinski, Phys. Rev. D 54 (1996) 1667.
- [53] R. Blumenhagen, B. Körs, D. Lüüst, J. High Ener. Phys. 0102 (2001) 030;  
Phys. Lett. B 532 (2002) 141.
- [54] F.G. Marchesano, *Intersecting D-brane models*, hep-th/0307252.
- [55] R. Blumenhagen, M. Cvetič, F. Marchesano, G. Shiu, J. High Ener. Phys. 0503 (2005) 050.  
R. Blumenhagen, B. Körs, D. Lüüst, T. Ott, Nucl. Phys. B 616 (2001) 3.
- [56] L.E. Ibáñez, F. Marchesano, R. Rabadan, J. High Ener. Phys. 0111 (2001) 002.
- [57] R. Blumenhagen, D. Lüüst, S. Stieberger, J. High Ener. Phys. 0307 (2003) 036.

- [58] G. Veneziano, S. Yankielowicz, Phys. Lett. B 113 (1982) 231.
- [59] M. Cvetič, P. Langacker, J. Wang, Phys. Rev. D 68 (2003) 046002.
- [60] P.G. Camara, A. Font, L.E. Ibáñez, J. High Ener. Phys. 0509 (2005) 013.
- [61] C.M. Chen, T. Li, D.V. Nanopoulos, Nucl. Phys. B 740 (2006) 79.
- [62] E. Dudas, C. Timirgaziu, Nucl. Phys. B 716 (2005) 65.
- [63] R. Blumenhagen, M. Cvetič, F. Marchesano, G. Shiu, J. High Ener. Phys. 0503 (2005) 050.
- [64] S. Forste, G. Honecker, *Rigid D6-branes on  $T^6/[Z_2 \times Z_{2M} \times \Omega\mathcal{R}]$  with discrete torsion*, arXiv:1010.6070 [hep-th].
- [65] C.M. Chen, T. Li, V.E. Mayes, D.V. Nanopoulos, Phys. Rev. D 78 (2008) 105015.
- [66] H. Fusaoka, Y. Koide, Phys. Rev. D 57 (1998) 3986.
- [67] G. Ross, M. Serna, Phys. Lett. B 664 (2008) 97.
- [68] S. Antusch, J. Kersten, M. Lindner and M. Ratz, Nucl. Phys. B **674**, 401 (2003) doi:10.1016/j.nuclphysb.2003.09.050 [hep-ph/0305273].
- [69] S. Antusch, J. Kersten, M. Lindner, M. Ratz and M. A. Schmidt, JHEP **0503**, 024 (2005) doi:10.1088/1126-6708/2005/03/024 [hep-ph/0501272].
- [70] J. Gemmill, E. Howington, and V. Mayes, To appear.
- [71] T. Li, J. A. Maxin, V. E. Mayes and D. V. Nanopoulos, Phys. Rev. D **94**, no. 2, 025002 (2016) doi:10.1103/PhysRevD.94.025002 [arXiv:1602.09099 [hep-ph]].